JETIR.ORG ISSN: 2349-5162 | ESTD Year : 2014 | Monthly Issue
JOURNAL OF EMERGING TECHNOLOGIES AND INNOVATIVE RESEARCH (JETIR)
An International Scholarly Open Access, Peer-reviewed, Refereed Journal

# AN ANALYSIS OF THE PERFORMANCE OF UNDERWATER WIRELESS OPTICAL COMMUNICATION SYSTEMS OVER A WIDE RANGE OF OPTICAL TURBULENCE

**Nakka Abbulu Pavan[1], Dr.Maruvada Sailaja[2]**
Department of Electronics and Communication,
University College of Engineering,
Jawaharlal Nehru technological University Kakinada Andhra Pradesh, India
nakkapavan1024@gmail.com[1]

## *Abstract*

***Three key degradation phenomena impact optical signal transmission under water: absorption, scattering, and turbulence. However, the statistical distribution of turbulence-induced fading is still poorly understood. In this paper, we evaluate the performance of underwater wireless optical communication (UWOC) systems in relation to well-known statistical distributions for optical turbulence such as lognormal, Gamma, K, Weibull, and exponentiated Weibull distributions in order to investigate the effect of different probability density functions (PDFs) proposed for the statistical behaviour of fading under water. For accuracy, we use a generic channel model with absorption and scattering effects that is based on the Monte Carlo (MC) numerical approach, and we treat the fading effect as a multiplicative coefficient with the aforementioned PDFs. We construct closed-form formulas for the average bit error rate (BER) and outage probability, as system performance measures, with regard to all of the channel degrading effects and the statistical distributions indicated above. Our findings show that as turbulence strength, as measured by the scintillation index value, increases, the gap between system performance predicted by different statistical distributions widens, and this gap manifests primarily as a change in the slope of average BER or outage probability curves versus average transmitted power per bit. This highlights the significance of precise channel models in the design of UWOC systems.***

***Keywords:*** *Underwater wireless optical communication (UWOC), temperature gradient, relaying, mixture models, Distributions, outage probability, bioterror rate (BER), ergodic capacity.*

## 1. Introduction

Underwater wireless optical communication (UWOC) is quickly becoming a prominent technique for high-throughput, high-data-volume underwater applications. In comparison to the well-established acoustic communication mechanism, the new alternative, i.e., optical transmission, can provide much higher data rates on the order of Gbps, significantly improved security due to the directionality of optical beams, lower time latency due to light's extremely faster propagation speed compared to acoustic waves, and better compatibility with the underwater ecosystem [1]. These unrivalled advantages have paved the way for exciting applications such as underwater sensor networking, monitoring, navigation, real-time video transmission, oil infrastructure maintenance and control, and so on, and have prompted extensive research efforts toward designing efficient UWOC systems that can facilitate underwater exploration and communication [2-5]. Comprehensive UWOC channel characterization study has revealed that optical signal transmission under water is impacted by three key degrading events, including absorption, scattering, and turbulence-induced fading [5-10]. These characteristics, when combined, make the UWOC channel a difficult environment to predict and restrict the greatest possible connection lengths to generally less than 100 m. As a result, recent research activity in this domain might be split into two groups. The first type of research activities attempts to model the channel impulse response appropriately with respect to all of the aforementioned impairing effects, such as absorption and scattering characterization in the form of a fading-free impulse response (FFIR) based on the Monte Carlo (MC) numerical method [5,11-13], and theoretical and experimental characterization of optical turbulence under water [10,14-16]. Other researchers, on the other hand, have focused on the intelligent and efficient design of transmission/reception techniques, such as multiple-input multiple-output (MIMO) transmission [17-19] and relay-assisted transmission [20-22], that can alleviate some of the channel impairments and improve system performance and viable link length. In the meanwhile, several intriguing experimental experiments have been completed as proof of concept to transfer theoretical advancements to the actual world. For example, in [23], the authors accomplished MIMO orthogonal frequency division multiplexing (OFDM) across UWOC channels experimentally. Furthermore, [24] demonstrated the feasibility of 5.5 Gbps transmission across a 26 m air-water optical wireless channel utilising OFDM modulation of a 520 nm laser diode. More intriguingly, [25]

experimentally demonstrated 12.4 Gbps high-speed underwater optical communication using blue laser diodes operating at 450 nm. The study presented in this work is an example of the first type of activity, which is an attempt to improve the channel model for UWOC systems. In this regard, [26,27] offered important theoretical and experimental research on the characterisation of optical beam propagation through water, focusing on absorption and scattering effects for various water types, whereas [9] accomplished the same for optical turbulence under water. The MC numerical approach was then used to model the FFIR of UWOC channels while accounting for absorption and scattering effects [5,7,8,11]. In addition, [5] presented a double gamma function for the channel FFIR to help with system analysis in terms of closed-form formulae. As a result, for the FFIR of MIMO UWOC lines with an arbitrary number of light sources and detectors, [12] suggested a weighted Gamma function polynomial. Many additional noteworthy research endeavours have focused on characterising underwater turbulence as the channel's third significant deteriorating influence. However, the majority of these publications are concerned with the theoretical research of irradiance variation and fading strength as a function of channel physical features and turbulence parameters. In this context, [28] used the Rytov technique to calculate an accurate power spectrum for the refractive index of UWOC channels. The scintillation index of planar and spherical optical waves travelling in turbulent UWOC channels was then calculated [10,29]. Furthermore, [30] calculated the on-axis scintillation index of a focussed Gaussian beam for light oceanic turbulence and assessed the system's average bit error rate (BER) with regard to the lognormal distribution for channel fading. Despite all of the above-mentioned excellent research endeavours, it is not yet clear whether the same statistical distributions that apply to free-space optics (FSO) also apply to UWOC channels. To the best of our knowledge, almost all of the reported works in the open literature use the same statistical distributions for UWOC channel fading, primarily the lognormal distribution, to evaluate the performance of such systems; however, the distribution of turbulence induced fading plays an important role in determining the performance of UWOC systems and accurately predicting their reliability. Motivated by this fact, [14,15] recently developed experimental setups to measure the fluctuated version of the received intensity through turbulent laboratory-scale UWOC links, which were affected by the presence of air bubbles and random temperature variations, and then evaluated the validity of different probability density functions (PDFs) in predicting the measured data in terms of their goodness of fit. Under this paper, we examine the performance of UWOC systems in a wide range of optical turbulence, as characterised by the scintillation index value, from weak to high, with the same purpose but from a different perspective. To acquire an accurate system performance, we first quantify the absorption and scattering effects using the MC numerical technique, and then treat the fading impact as a multiplicative coefficient using certain well-known optical turbulence distributions. Then, as system performance metrics, we develop closed-form formulas for the average BER and outage probability with regard to all of the channel degrading effects and the aforementioned statistical distributions. The remainder of the paper is structured as follows. Section 2 provides an introduction of UWOC channel modelling and discusses our system model for underwater communication using on-off keying (OOK) intensity modulation/direct detection (IM/DD). Section 3 describes the statistical distributions under consideration and explains how their constant parameters can be derived. In Section 4, we develop the average BER and outage probability formulae, which will be employed in Section 5 for numerical results and computer simulations. Finally, Section 6 brings the paper to a close.

## 2. Models of channels and systems

### *2.1. Modelling of UWOC channels*

Each photon in the propagating optical beam across the UWOC channel interacts with water molecules and suspended particles, which is described as absorption and scattering. In reality, during the absorption process, the energy of each photon is thermally dissipated; this is denoted by the absorption coefficient a(, where is the wavelength). Furthermore, throughout the scattering process, the direction of each photon can be modified, which is represented by the scattering coefficient $b(\lambda)$. While the absorption process only causes a loss in received optical power, the scattering process causes both temporal spread of the received optical signal (because different components of the propagating light beam may arrive at different time instances to the receiver) and attenuation of the received optical power (because some of the scattered photons may deviate from the propagation path). The total energy loss of non-scattered light, due to absorption and scattering, can be characterized by extinction coefficient $c(\lambda) = a(\lambda) + b(\lambda)$. The value of these parameters $a(\lambda)$ and $b(\lambda)$ varies with the water type and the wavelength used $\lambda$, and have their minimum values at the interval 400 nm < $\lambda$ < 530 nm [27]; As a result, UWOC systems communicate using the blue/green part of the visible light spectrum. According to the detailed investigations in [4,5,7,8] on the channel modelling of UWOC channels and complete MC simulations, the FFIR of UWOC channels, which includes absorption and scattering effects, cannot be simply represented as a loss coefficient like FSO connections. The large amount of multiple scattering on the propagating light wave, depending on the water type and diffusivity of the source beam and field of view (FoV) of the receiver, significantly spreads the received optical signal in the temporal domain, such that, for the required high data transmission rates on the order of Gbps, the delay spread of the channel is comparable with or even larger than the bit duration time, leading to a potential inter-symbol irradiation (ISI). Although the channel FFIR may be easily constructed as closed-form functions similar to [5,12], for the purpose of generality and accuracy, we simulate the UWOC channel based on the MC technique in a similar way to [4,5,7,8] and indicate the result with h0(t) throughout our study. Optical turbulence, on the other hand, arises as a result of random changes in the refractive index caused by temperature and salinity oscillations in the water [31]. In order to take into account, the turbulence induced fading effects as well, we multiply the FFIR of the channel $h0(t)$ by a positive multiplicative fading coefficient $\tilde{h}$ in a similar approach to [17,18,32,33]. The PDF of h can vary depending on the range of optical turbulence, from weak to strong, as detailed in the next section. Extensive research has been conducted in recent years on the theoretical characterisation of turbulence strength under water, as measured by scintillation index, and on the relationship between this metric and the physical characteristics and turbulence parameters of the UWOC channel [28,10,29,30]. The scintillation index of a light wave with instantaneous intensity $I = I0\tilde{h}$ is defined as

$$\sigma_I^2 = \frac{\mathbb{E}[I^2] - \mathbb{E}^2[I]}{\mathbb{E}^2[I]} = \frac{\mathbb{E}[\tilde{h}^2] - \mathbb{E}^2[\tilde{h}]}{\mathbb{E}^2[\tilde{h}]}. \quad (1)$$

where $I0$ is the fading-free intensity, and E[$x$] denoted the expected value of the random variable $x$. [10, Eqs. (1) (8)] has detailed mathematical formulations of the scintillation index for optical plane and spherical waves under the assumption of weak oceanic turbulence. The scintillation index is commonly used to distinguish between the weak and strong turbulence regimes, i.e., when this parameter is less than unity, the channel is regarded as weak turbulence, and vice versa.

### *2.2. Model of the OOK IM/DD UWOC system*

We employ OOK modulation in this research for performance analysis; hence, the transmitter's transmitted data sequence may be written as

$$S(t) = \sum_{k=-\infty}^{\infty} b_k P(t - kT_b), \quad (2)$$

where $bk \in \{0, 1\}$ is the $k$th time slot transmitted bit, $Tb = 1/Rb$ is the bit duration time, $Rb$ is the data transmission rate, and $P(t - kTb)$ is the $k$th time slot transmitted optical signal with the average power of $2Pb$, where $Pb$ is the average transmitted power per bit of the transmitter. The received signal is then represented as

$$y(t) = S(t) * h(t) = \tilde{h} \sum_{k=-\infty}^{\infty} b_k I(t - kT_b), \quad (3)$$

in which $h(t) = \tilde{h}h0(t)$ is the channel aggregated impulse response, $I(t) = P(t) * h0(t)$, and $*$ denotes the convolution operator. We should highlight that, for simplicity's sake, we use symbol-by-symbol detection, which is suboptimal in the presence of ISI, which means that the receiver integrates over each Tb second to acquire the photodetector's integrated current. [4] provides a generalisation to UWOC systems with multiple symbol detection (MSD). Furthermore, in the integrated version of the received signal, numerous noise components such as signal-dependent shot noise, background light, dark current, and thermal noise arise. These noise components may be represented as an analogous noise component with Gaussian distribution due to their additivity and independence [34]. Furthermore, we assume that the signal dependent shot noise has no influence in comparison to the other noise components (see the appendix of [18]), and hence the noise variance is independent of the incoming optical signal intensity.

## 3. Under discussion are statistical distributions

This section provides a brief overview of the well-known statistical distributions in the setting of optical turbulence that we will use in this work to assess their efficacy in forecasting underwater turbulence-induced fading. We also show how the constant parameters of each of the PDFs under consideration are connected to the scintillation index value, and hence to the physical properties of the underwater turbulent channel. More precisely, we assume that a set of turbulence settings for the UWOC channel is provided, resulting in a certain scintillation index value. As a result, the constant parameters of each of the investigated PDFs should be set so that two equalities hold. The first is fading normalisation equality, which means that the fading coefficients are normalised so that they neither amplify nor attenuate the incoming optical signalize., E[$\tilde{h}$] = 1. And the second is the *scintillation index equality*, i.e., $\sigma 2\ I = \sigma 2\ I,g$, where $\sigma 2\ I$ is the predicted scintillation index value by the considered PDF based on Eq. (1), and $\sigma 2\ I,g$ is a value for the turbulent channel's scintillation index depending on the physical specifications of the UWOC link.

### *3.1. Lognormal distribution*

Because of its simplicity, lognormal is the most commonly employed statistical distribution in recent years to describe underwater optical turbulence. The lognormal distribution captures the variations caused by mild air turbulence well. It is characterized by $\sigma 2\ I < 1$ [33,32,35]. In this case, the channel fading coefficient $\tilde{h} = \exp(2X)$ has the PDF.

$$f_{\tilde{h}}(\tilde{h}) = \frac{1}{2\tilde{h}\sqrt{2\pi\sigma_X^2}} \exp\left(-\frac{\left(\ln(\tilde{h}) - 2\mu_X\right)^2}{8\sigma_X^2}\right), \quad (4)$$

where $X = 1/2 \ln(\tilde{h})$ denotes the fading log-amplitude which has a Gaussian distribution with mean $\mu X$ and variance $\sigma 2\ X$ [33]. It is easy to verify that *fading normalization equality* for lognormal distribution leads to the relation $\mu X = -\sigma 2\ X$ between the log-amplitude mean and variance [33,35]. Therefore, lognormal distribution is a function of a single parameter $\sigma 2\ X$ that can be obtained using *scintillation index equality* for the given scintillation index value as $\sigma 2\ X = 0.25 \ln(1 + \sigma 2\ I,g)$ [17].

### *3.2. Gamma distribution*

The gamma distribution, which was proposed in [15] as a contender for characterising UWOC fading, with shape parameter $k$ and scale parameter $\theta$ can be expressed as

$$f_{\tilde{h}}(\tilde{h}) = \frac{1}{\Gamma(k)\theta^k} \tilde{h}^{k-1} \exp(-\tilde{h}/\theta), \quad (5)$$

in which $\Gamma(k)$ denotes the Gamma function. For the Gamma distribution expressed in (5) we can obtain E[$\tilde{h}$] = $k\theta = 1$ and E[$\tilde{h}2$] = $k(k + 1)\theta 2$. Hence, the constant parameters of Gamma distribution can easily be obtained for the given scintillation index value as $\theta = 1/k = \sigma 2\ I,g$.

### *3.3. K distribution*

The PDF of the K distribution, which was primarily utilised in optical turbulence literature to describe significant fading in FSO links specified by $\sigma 2\ I \geq 1$, is given by [36];

$$f_{\tilde{h}}(\tilde{h}) = \frac{2\alpha}{\Gamma(\alpha)} (\alpha\tilde{h})^{(\alpha-1)/2} K_{\alpha-1}\left(2\sqrt{\alpha\tilde{h}}\right), \quad (6)$$

in which $K\Gamma(x)$ is the $\Gamma$th-order modified Bessel function of the second kind, and $\alpha$ is a positive parameter relating to the given scintillation index value as $\alpha = 2/(\sigma 2\ I,g - 1)$.

### *3.4. Weibull distribution*

In recent experimental research [15,37], the Weibull distribution was utilised to represent the UWOC turbulence effect in a laboratory-scale setting with extremely mild fading. Previously, the Weibull distribution was employed to quantify atmospheric turbulence in [38]. The Weibull distribution's PDF is given by

$$f_{\tilde{h}}(\tilde{h}) = \frac{\beta}{\eta} (\tilde{h}/\eta)^{\beta-1} \exp\left(-(\tilde{h}/\eta)^{\beta}\right) \quad (7)$$

where $\beta$ and $\eta$ are the constant shape parameters. For the given PDF in (7) we can obtain E[$\tilde{h}$] = $\eta\Gamma(1 + 1/\beta)$ and E[$\tilde{h}2$] = $\eta 2\Gamma(1 + 2/\beta)$. Consequently, we can derive the value of $\beta$ for a given scintillation index value by solving the equation Then it is easy to obtain the value of $\eta$ as $\eta = 1/\Gamma(1 + 1/\beta)$.

$$\sigma_{I,g}^2 = \left[\Gamma(1 + 2/\beta)/\Gamma^2(1 + 1/\beta)\right] - 1. \quad (8)$$

### *3.5. Exponentiated Weibull distribution*

In [38], the exponentiated Weibull distribution was utilised to characterise the fading in FSO connections for a wide range of turbulence. The PDF of the exponentiated Weibull distribution with parameters, and is given by

$$f_{\tilde{h}}(\tilde{h}) = \frac{\alpha\beta}{\eta} (\tilde{h}/\eta)^{\beta-1} \exp\left(-(\tilde{h}/\eta)^{\beta}\right) \times \left[1 - \exp\left(-(\tilde{h}/\eta)^{\beta}\right)\right]^{\alpha-1}. \quad (9)$$

To approximate the parameter values for the exponentiate Weibull distribution, we may use the findings from a fitting approach in [38] as;

$$\alpha = \frac{7.22\sigma_{I.g}^{2/3}}{\Gamma(2.487\sigma_{I.g}^{2/6} - 0.104)}, \quad (10)$$

$$\beta = 1.012(\alpha\sigma_{I.g}^2)^{-13/25} + 0.142, \quad (11)$$

$$\eta = \frac{1}{\alpha\Gamma(1+1/\beta)g_1(\alpha,\beta)}, \quad (12)$$

in which $gn(\alpha, \beta)$ is a series defined as

$$g_n(\alpha,\beta) = \sum_{i=0}^{\infty} \frac{(-1)^i\Gamma(\alpha)}{i!(i+1)^{1+n/\beta}\Gamma(\alpha-i)}. \quad (13)$$

According to the reasoning in [37], because of the fast convergence speed of (13), the infinite sequence of $gn(\alpha, \beta)$ can acceptably be approximated using the first 10 terms.

## 4. Performance evaluation

### *4.1. Average BER*

Using (3), the 0th time slot integrated current of the receiver can be expressed as; where $u(s) = R\int_0^{Tb} I(t)dt$, $u(I,k) = R\int_0^{Tb} I(t-kTb)dt = R\int_{-(k-1)Tb}^{-kTb} I(t)dt$, and $R = \eta q/hf$ is the photodetector's responsivity.

$$r_{b_0} = b_0\tilde{h}u^{(s)} + \tilde{h}\sum_{k=-L}^{-1} b_k u^{(I,k)} + v_{T_b}, \quad (14)$$

Furthermore, $\eta$, $q$, $h$, $f$, and $L$ are the photodetector's quantum efficiency, electron's charge, Planck's constant, optical source frequency, and channel memory, respectively. In this notation, $u(I,k\neq0)$ specifies the ISI effect while $u(I,k=0)$ refers to the desired signal contribution, i.e., $u(I,k=0) = u(s)$ [17]. Moreover, $vTb$ is the receiver Gaussian-distributed integrated noise component with mean zero and variance $\sigma 2\ Tb$. Similar to [17], we adopt the same fading coefficients for all of the consecutive bits in (14) due to the much larger coherence time of the channel compared to the typical data rates [14,31]. Assuming that the channel state information (CSI) is available to the receiver, the integrated current over each $Tb$ seconds will be compared with the threshold value of $\tilde{h}u(s)/2$. Then the probabilities of error, conditioned on the transmission of ''1'' and ''0'' at the 0th time slot, can be obtained respectively as

$$P_{be|1,\tilde{h},b_k} = \Pr(r_{b_0} \le \tilde{h}u^{(s)}/2 | b_0 = 1) = Q\left(\frac{\tilde{h}\left[u^{(s)}/2 + \sum_{k=-L}^{-1} b_k u^{(I,k)}\right]}{\sigma_{T_b}}\right), \quad (15)$$

$$P_{be|0,\tilde{h},b_k} = \Pr(r_{b_0} \ge \tilde{h}u^{(s)}/2 | b_0 = 0) = Q\left(\frac{\tilde{h}\left[u^{(s)}/2 - \sum_{k=-L}^{-1} b_k u^{(I,k)}\right]}{\sigma_{T_b}}\right), \quad (16)$$

where $Q(x) = (1/\sqrt{2\pi})\int_x^\infty \exp(-y2/2)dy$ is the Gaussian Q-function [17]. Then the final BER can be obtained by averaging over fading coefficient $\tilde{h}$ as well as all $2L$ possible data sequences for $bk$'s as

$$P_{be} = \frac{1}{2^{L+1}}\sum_{b_k}\int_0^\infty \left[P_{be|1,\tilde{h},b_k} + P_{be|0,\tilde{h},b_k}\right] f_{\tilde{h}}(\tilde{h})d\tilde{h}. \quad (17)$$

In the next section, we will obtain the closed form equations for the average BER in (17), we denote by $Pbe|b0,bk$ the averaged version of the conditional BERs in (15) and (16) over the channel fading $\tilde{h}$ for $b_0 = 1$ and 0, respectively, i.e.,

$$P_{be|b_0,b_k} = \int_0^\infty P_{be|b_0,\tilde{h},b_k} f_{\tilde{h}}(\tilde{h})d\tilde{h} = \int_0^\infty Q\left(C_{b_0}\tilde{h}\right) f_{\tilde{h}}(\tilde{h})d\tilde{h}, \quad (18)$$

where $Cb_0$ is the constant coefficient of the Gaussian Q-functions in (15) and (16), i.e.,

$$C_{b_0} = \frac{\left[u^{(s)}/2 + (-1)^{b_0+1}\sum_{k=-L}^{-1} b_k u^{(I,k)}\right]}{\sigma_{T_b}}. \quad (19)$$

In Section 3, we present closed-form formulations for Pbe|b0,bk in Eq. (18) with regard to the statistical distributions studied. The closed-form formula for the average BER may therefore be found using (17) as

$$P_{be} = \frac{1}{2^{L+1}}\sum_{b_k}\left[P_{be|1,b_k} + P_{be|0,b_k}\right]$$

#### *4.1.1. Lognormal distribution*

In the case of lognormal distribution, $Pbe|b0,bk$ in (18) can effectively be calculated using Gauss–Hermite quadrature formula [39, Eq. (25.4.46)] as

$$P_{be|b_0,b_k} = \int_0^\infty Q\left(C_{b_0}\tilde{h}\right)\frac{1}{2\tilde{h}\sqrt{2\pi\sigma_X^2}}\exp\left(-\frac{(\ln(\tilde{h}) - 2\mu_X)^2}{8\sigma_X^2}\right)d\tilde{h} = \frac{1}{\sqrt{\pi}}\int_{-\infty}^\infty Q\left(C_{b_0}\exp\left[2\mu_X + 2y\sqrt{2\sigma_X^2}\right]\right)e^{-y^2}dy \approx \frac{1}{\sqrt{\pi}}\sum_{i=1}^n w_i Q\left(C_{b_0}\exp\left[2\mu_X + 2y_i\sqrt{2\sigma_X^2}\right]\right), \quad (20)$$

where $n$ is the order of approximation and $yi$ is the $i$th zero of the $n$th-order Hermite polynomial, $Hn(y)$. Moreover, $wi$, $i = 1, 2..., n$, are weights of the $n$th-order approximation given by [39], Numerical values for $wi$'s and $yi$'s can be found in [39, Table 25.10].

$$w_i = \frac{2^{n-1}n!\sqrt{\pi}}{n^2\left[H_{n-1}(y_i)\right]^2}. \quad (21)$$

#### *4.1.2. Gamma distribution*

In the case of the Gamma distribution, the Laguerre polynomial approximation can be used. [39, Eq. (25.4.45)] to approximate $Pbe|b0,bk$ in (18) as

$$P_{be|b_0,b_k} = \int_0^\infty Q\left(C_{b_0}\tilde{h}\right)\frac{1}{\Gamma(k)\theta^k}\tilde{h}^{k-1}\exp(-\tilde{h}/\theta)\,d\tilde{h} = \frac{1}{\Gamma(k)}\int_0^\infty Q\left(C_{b_0}\theta x\right)x^{k-1}e^{-x}dx \approx \frac{1}{\Gamma(k)}\sum_{i=1}^n v_i Q\left(C_{b_0}\theta x_i\right)x_i^{k-1}, \quad (22)$$

where $n$ is again the order of approximation and $xi$ is the $i$th zero of the $n$th-order Laguerre polynomial, $Ln(x)$. Furthermore, $vi$, $i = 1, 2..., n$, are weights of the $n$th-order approximation given by [39] Numerical values for $v_i$'s and $x_i$'s can also be found in [39, Table 25.9].

$$v_i = \frac{(n!)^2 x_i}{(n+1)^2\left[L_{n+1}(x_i)\right]^2}. \quad (23)$$

#### *4.1.3. K distribution*

When the channel fading follows the K distribution, we may use Meijer G-functions to get the closed form of $Pbe|b0,bk$ (18). In this case, we can first use [40, Eq. (8.4.23.1)] to express the second-order l thrower modified Bessel function in terms of the Meijer G-function as

$$K_l(x) = \frac{1}{2}G_{0,2}^{2,0}\left[x^2/4\middle|_{l/2,-l/2}^{-}\right]. \quad (24)$$

The Gaussian Q-function is then connected to the complementary error function erfc(.) by $\text{erfc}(x) = 2Q(\sqrt{2}x)$. As a result, we can rewrite (18) for K distributed fading as

$$P_{be|b_0,b_k} = \int_0^\infty \frac{1}{2}\text{erfc}\left(\frac{C_{b_0}}{\sqrt{2}}\tilde{h}\right)\frac{2\alpha}{\Gamma(\alpha)}(\alpha\tilde{h})^{(\alpha-1)/2}K_{\alpha-1}\left(2\sqrt{\alpha\tilde{h}}\right)d\tilde{h}. \quad (25)$$

Using [40, Eq. (8.4.14.2)] to write $\text{erfc}(\sqrt{x}) = \sqrt{1\pi}\,G2,01,2[x|10,1/2]$, [41, Eq.(21)], and (24), we can express the closed form of (25) as

$$P_{be|b_0,b_k} = \frac{2^{\alpha-2}}{\sqrt{\pi^3}\Gamma(\alpha)}G_{5,2}^{2,4}\left[\frac{8C_{b_0}^2}{\alpha^2}\middle|_{0,1/2}^{\frac{1-\alpha}{2},\frac{2-\alpha}{2},0,\frac{1}{2},1}\right]. \quad (26)$$

#### 4.1.4. Weibull and exponentiated Weibull distributions

The Laguerre polynomial approximation [39, Eq. (25.4.45)] is used. we can calculate $Pbe|b0,bk$ in (18) for the exponentiated Weibull distribution as

$$\begin{aligned} P_{be|b_0,b_k} &= \int_0^\infty Q\left(C_{b_0}\tilde{h}\right)\frac{\alpha\beta}{\eta}(\tilde{h}/\eta)^{\beta-1}\exp\left(-(\tilde{h}/\eta)^{\beta}\right) \\ &\quad\times\left[1-\exp\left(-(\tilde{h}/\eta)^{\beta}\right)\right]^{\alpha-1}d\tilde{h} \\ &= \int_0^\infty Q\left(C_{b_0}\eta x^{1/\beta}\right)\alpha e^{-x}\left[1-e^{-x}\right]^{\alpha-1}dx \\ &\approx \sum_{i=1}^{n}\alpha v_i Q\left(C_{b_0}\eta x_i^{1/\beta}\right)e^{-x_i}\left[1-e^{-x_i}\right]^{\alpha-1}, \end{aligned} \tag{27}$$

where $n$, $vi$, and $xi$ are defined in Section 4.1.2. Note that Weibull distribution is a special case of exponentiated Weibull for $\alpha$ = 1. Therefore, in the case Weibull distribution, (27) simplifies to $Pbe|b0,bk \approx \Sigma ni=1\alpha viQ(Cb0\eta xi/\beta i)e-xi$.

### 4.2. Outage probability

The outage probability is defined as the likelihood of the channel capacity falling below a pre-set rate target, which is similar to the probability of the receiver instantaneous signal-to-noise ratio falling below a predefined threshold (SNR) $\gamma$ being below a certain threshold $\gamma th$ [35], i.e.,

$$P_{\text{out}} = \Pr(\gamma < \gamma_{th}). \tag{28}$$

Before calculating the system outage probability, an adequate specification of the electrical SNR formula for the UWOC ISI channel is necessary, according to (28). Recently, depending on how ISI is addressed, two distinct definitions for instantaneous electrical SNR in UWOC channels have been stated in [22]. The initial definition, in particular, interpreted the ISI term in (14) as noise and defined as the effective electrical signal-to-interference-plus-noise ratio (SINR) as

$$\gamma = \frac{\left[\tilde{h}u^{(s)}\right]^2}{\left[\tilde{h}\sum_{k=-L}^{-1}b_k u^{(I,k)}\right]^2+\sigma_{T_b}^2}. \tag{29}$$

The second formulation, on the other hand, derives the instantaneous SNR formula from the relationship between and the conditional BER, which is specified as (15) and (16), respectively.

$$\gamma = \frac{\tilde{h}^2\left[u^{(s)}+(-1)^{b_0+1}\sum_{k=-L}^{-1}2b_k u^{(I,k)}\right]^2}{\sigma_{T_b}^2}. \tag{30}$$

Extensive numerical studies in [22] for varied UWOC channel circumstances indicated the same performance for both electrical SNR definitions in Eqs. (29) and (29). (30). As a result, for the purpose of brevity, we will only discuss the first definition of the electrical SNR, which interprets the ISI degrading impact as noise. In this situation, the UWOC system outage probability is as follows:

$$\begin{aligned} P_{\text{out}} &= \frac{1}{2^L}\sum_{\{b_k\}}\Pr\left(\tilde{h}\le\mathcal{T}\right) \\ &= \frac{1}{2^L}\sum_{\{b_k\}}F_{\tilde{h}}(\mathcal{T}), \end{aligned} \tag{31}$$

in which $\tilde{F}h$(.) is the cumulative distribution function (CDF) of the nonnegative random variable (RV) $\tilde{h}$, and the constant parameter , based on (29), is defined as

$$\mathcal{T} = \sqrt{\frac{\gamma_{th}\sigma_{T_b}^2}{\left[u^{(s)}\right]^2-\gamma_{th}\left[\sum_{k=-L}^{-1}b_k u^{(I,k)}\right]^2}}. \tag{32}$$

The form of the outage probability formula in (31) implies that characterising the closed forms of the outage probability with respect to the various statistical distributions considered in Section 3 necessitates analytical formulation of the CDF of the corresponding PDFs, which will be done in the remainder of this section. We can obtain the CDF for the lognormal UWOC channel in particular as

$$\begin{aligned} F_{\tilde{h}}(\mathcal{T}) &= \Pr\left(e^{2X}\le\mathcal{T}\right) \\ &= 1-Q\left(\frac{\ln(\mathcal{T})+2\sigma_X^2}{2\sigma_X}\right). \end{aligned} \tag{33}$$

The CDF of a Gamma-distributed RV, on the other hand, is widely known to be provided by

$$F_{\tilde{h}}(\mathcal{T}) = \frac{1}{\Gamma(k)}\gamma(k,\mathcal{T}/\theta), \tag{34}$$

where $\gamma(\cdot,\cdot)$ is the lower incomplete gamma function. Furthermore, using (24) and [40, Eq. (2.24.2.2)], we can obtain the CDF of a K distributed RV as

$$F_{\tilde{h}}(\mathcal{T}) = \frac{1}{\Gamma(\alpha)}G_{1,3}^{2,1}\left[\alpha\mathcal{T}\Big|_{\alpha,1,0}^{1}\right]. \tag{35}$$

Finally, for the exponentiated Weibull distribution the CDF of $\tilde{h}$ is given by [38, Eq. (15)]

$$F_{\tilde{h}}(\mathcal{T}) = \left[1-\exp\left(-(\tilde{h}/\eta)^{\beta}\right)\right]^{\alpha}, \tag{36}$$

which implies that for the Weibull distribution $\tilde{F}h$ ( (□ ) = 1 − exp−$(\tilde{h}/\eta)\beta$). This complete Section 3's closed-form characterisation of the UWOC outage probability in relation to the statistical distributions discussed.

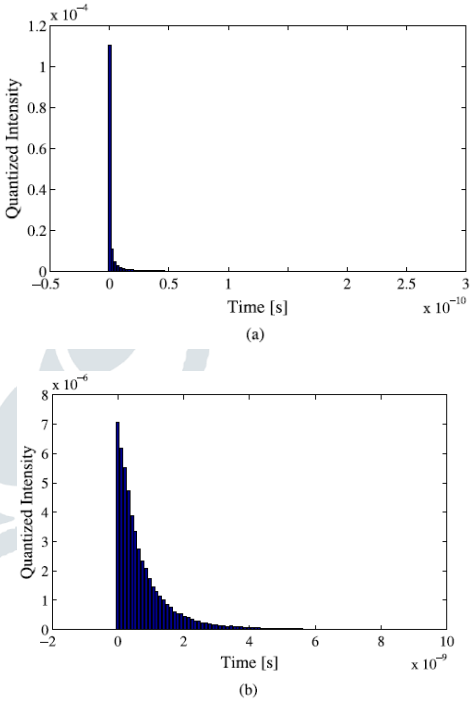


**Fig. 1.** FFIR measurements of two sample point-to-point UWOC links: (a) a 25 m laser-based collimated UWOC connection in coastal waters; and (b) a 6 m LED-based diffusive UWOC link in murky harbour waters.

## 5. Statistical Findings

We present numerical results for the average BER and outage probability of UWOC systems across a wide range of turbulence specified by various statistical distributions for channel fading in this section. To ensure that the findings are as precise as possible, we use MC numerical calculations to account for absorption and scattering effects. We analyse coastal and turbid harbour water linkages with (a, b) = (0.179, 0.219) and (0.366, 1.824) m1 absorption and scattering coefficients, respectively [27]. Then we simulate the channel FFIR for both laser-based collimated and LED-based diffusive connections using the same approach as

[4,5,7] and the same typical system parameter values as [4]. Table 1 lists some of the key parameters utilised in the channel simulation. The temporal-domain FFIR of a 25 m laser-based collimated UWOC connection in coastal waters and a 6 m LED-based diffusive UWOC link in turbid harbour waters are shown in Figs. 1(a) and (b), respectively.

**Table 1**
Parameters used for the FFIR simulation and noise characterization.

| Coefficient | Value |
|---|---|
| Source wavelength, $\lambda$ | 532 nm |
| Semi-angle at half power of LED, $\theta_{1/2}$ | 15° |
| Laser half divergence angle, $\theta_{div}$ | 0.75 mrad |
| Laser beam waist radius, $W_z$ | 1 mm |
| Total number of transmitted photons for MC simulation, $N_t$ | $10^8$ |
| Water refractive index, $n$ | 1.331 |
| Receiver half angle FOV, $\theta_{FOV}$ | 40° |
| Aperture diameter, $D_0$ | 20 cm |
| Photon weight threshold at the receiver, $W_{th}$ | $10^{-6}$ |
| Quantum efficiency, $\eta$ | 0.8 |
| Optical filter transmissivity, $T_F$ | 0.8 |
| Optical filter bandwidth, $\Delta\lambda$ | 10 nm |
| Equivalent temperature, $T_e$ | 290 K |
| Load resistance, $R_L$ | 100 Ω |
| Dark current, $I_{dc}$ | $1.226 \times 10^{-9}$ A |
| Downwelling irradiance, $E$ | 1440 W/m$^2$ |
| Underwater reflectance of the downwelling irradiance, $R_d$ | 0.0125 |
| Viewing angle, $\phi_v$ | 90° (horizontal) |
| Directionality-dependence factor of underwater radiance, $L_{fac}$ | 2.9 |
| Water depth, $D_w$ | 30 m |

For each of these images, we first split the time gap between the latest and earliest detected photons into 80 bins, and then computed the normalised sum of all detected photon weights to the total number of transmitted photons for each bin. When these numbers are compared, they reveal that as water turbidity increases, so does channel loss and delay spread. Furthermore, LED-based transmission increases channel diffusivity, and so channel loss and temporal dispersion. As a result, the channel quality of a 6 m LED-based turbid harbour connection is poorer than that of a 25 m laser-based coastal link. The remainder of this section examines the performance of various UWOC connection topologies under a wide variety of optical turbulence characterised by different statistical distributions discussed in Section 3. The average BER of a 6mLED-based turbid harbour water connection with a scintillation index value of is shown in Fig. 2. $\sigma 2\ I = 0.2$ and the data transmission rate of $Rb = 200$ Mbps for various statistical distributions. As can be seen, different statistical distributions have varying results for system performance. The same behaviour is observed in Fig. 3 for the outage probability of the system with the same parameters and the threshold SNR value of $\gamma th$ = 25. According to the MC simulation findings in Fig. 1, laser-based transmission has much lower attenuation and temporal spread than LED-based transmission. The same result applies to coastal water linkages as opposed to turbid harbour water links with higher water turbidity. As shown in Fig. 1, these factors combine to produce much higher channel quality for laser-based coastal water connections than for LED-based turbid harbour water links, allowing laser-based coastal water links to have a greater communication range and data transfer rate. As a result, in Figures 4 and 5, we examine the average BER and outage probability of a 25 m laser-based coastal water connection with $\sigma 2\ I = 0.8$, $Rb = 1$ Gbps, and $\gamma th$ = 25, for various statistical distributions.

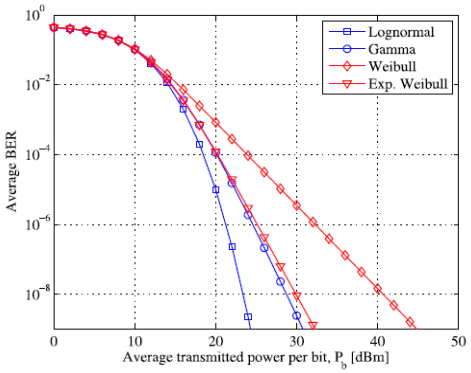


**Fig. 2.** A 6 m LED-based turbid harbour connection with an average BER of $\sigma 2\ I = 0.2$ and Rb = 200 Mbps data transfer rate for various statistical distributions.

To further see the fading strength impact, we ran the simulations in Figs. 6 and 7 with greater scintillation index values. i.e., $\sigma 2\ I = 2$. As predicted, the discrepancy between the outcomes of different statistical distributions grows as the scintillation index value increases under harsher fading conditions. As a result, given a value for the scintillation index of the UWOC channel, the expected system performance utilising alternative statistical distributions for UWOC channel fading will be vastly different. Exponentiated Weibull distribution is thought to fit actual measurement data over a wide range of optical turbulence, according to thorough experimental research in [16]. Based on this fact and our extensive simulation findings in this study, we can claim that the lognormal distribution always underestimates the turbulence strength because it performed better than the exponentiated Weibull in all of our simulation results. Furthermore, the Weibull and K distributions always overstate turbulence strength since they perform worse than the real performance achieved by exponentiating the Weibull distribution.

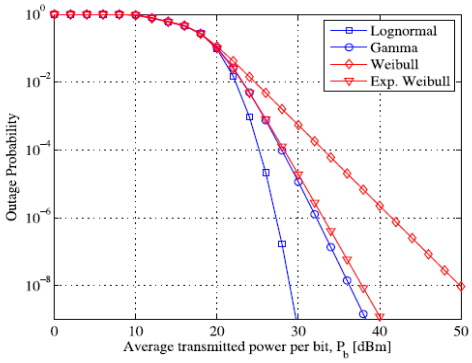


**Fig. 3.** The likelihood of a 6 m LED-based turbid harbour water connection failing with $\sigma 2\ I = 0.2$, $Rb = 200$ Mbps, and the threshold SNR of $\gamma th$ = 25 for various statistical distributions.

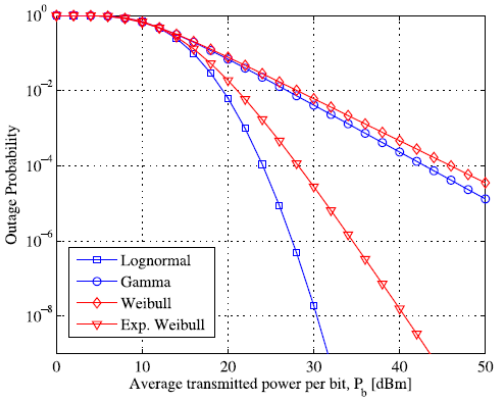


**Fig. 4.** The likelihood of a 25 m laser-based coastal water connection failing with $\sigma 2\ I = 0.8$, $Rb = 1$ Gbps, and $\gamma th$ = 25 for various statistical distributions.

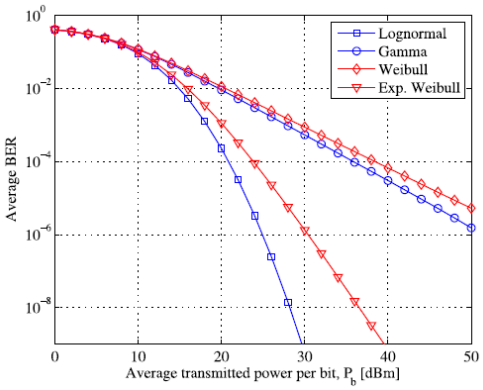


**Fig. 5.** A 25 m laser-based coastal water connection with an average BER of $\sigma 2\ I = 0.8$ and $Rb = 1$ Gbps for various statistical distributions.

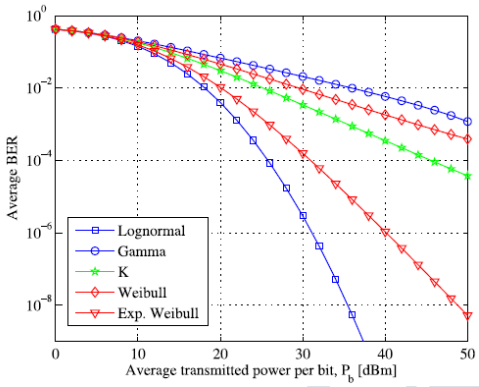


**Fig. 6.** The average BER of a 25 m laser-based coastal water connection with $\sigma 2\ I = 2$ and $Rb = 1$ Gbps for various statistical distributions.

derived by the exponentiated Weibull distribution Finally, except for the weak fading regime conducted over the scintillation index value of 0.2 in our Figs. 2 and 3, when Gamma distribution may give almost the same performance as exponentiated Weibull, Gamma distribution overestimates system performance. This demands more theoretical and practical research on the UWOC channel fading statistics. For UWOC fading, a robust theoretical method based on statistical optics and Karhunen-Loeve expansions is required, comparable to that of [42]. Furthermore, the difference between the findings of different PDFs is shown mostly in the shifting slope of average BER or outage probability curves vs average transmitted power per bit. This inspires another idea for future experimental studies: given a set of experimental data obtained by measuring the received irradiance through the turbulent UWOC channel, it is not necessary to keep the scintillation index value of the proposed PDFs the same as the scintillation index value of the measured experimental data. Instead, an optimization method may be necessary to acceptably fit the suggested PDF to the histogram of the measured data, which no longer results in the proposed PDF having the same scintillation index value as the observed experimental data.

## 6. Conclusion

In this paper, we studied the performance of point-to-point UWOC links under a wide range of optical turbulence, from weak to strong, as defined by the scintillation index value, in order to better investigate the statistics of turbulence-induced fading in underwater wireless optical communication (UWOC) channels. To account for the turbulence effect, we used the Monte Carlo numerical method to properly consider the absorption and scattering effects, and then multiplied the resulting fading free impulse response (FFIR) by a multiplicative fading coefficient described by some well-known statistical distributions in the optical turbulence literature. As system performance measures, we offered closed-form equations for calculating average BER and outage probability.

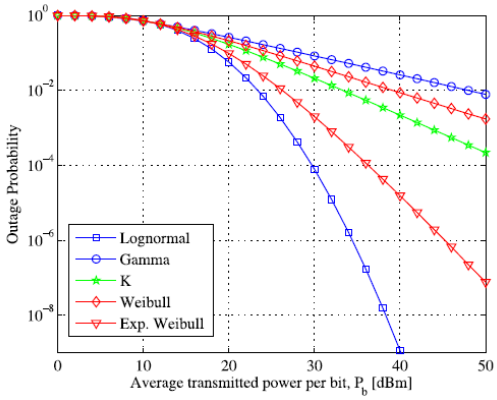


**Fig. 7.** The likelihood of a 25 m laser-based coastal water connection failing with $\sigma 2\ I = 2$, $Rb = 1$ Gbps, and $\gamma th = 25$ for various statistical distributions.

For increasing levels of the channel scintillation index, our detailed numerical studies revealed a wider gap between the performance outcomes predicted by different fading distributions. Furthermore, we discovered that the aforementioned difference manifests mostly as a change in the slope of average BER or outage probability curves vs average transmitted power per bit. This inspires a further idea for future experimental studies to obtain the constant parameters of different PDFs via an optimization procedure that appropriately fits the proposed distribution to the histogram of the experimental measured data, which no longer necessarily holds the scintillation index equality.

## References

[1] F. Akhoundi, M.V. Jamali, N. Banihassan, H. Beyranvand, A. Minoofar, J.A. Salehi, Cellular underwater wireless optical CDMA network: Potentials and challenges, IEEE Access 4 (2016) 4254–4268.

[2] F. Hanson, S. Radic, High bandwidth underwater optical communication, Appl. Optics 47 (2) (2008) 277 283.

[3] J.W. Giles, I.N. Bankman, Underwater optical communications systems. Part 2: basic design considerations, in: IEEE Military Communications Conference, 2005, MILCOM 2005, IEEE, 2005, pp. 1700–1705.

[4] M.V. Jamali, P. Nabavi, J.A. Salehi, MIMO underwater visible light communications: Comprehensive channel study, performance analysis, and multiple-symbol detection, IEEE Trans. Veh. Technol. (2018). [Online]. Available: https://ieeexplore.ieee. org/document/8365815/.

[5] S. Tang, Y. Dong, X. Zhang, Impulse response modelling for underwater wireless optical communication links, IEEE Trans. Commun. 62 (1) (2014) 226–234.

[6] N.B. Mehta, J.Wu, A.F. Molisch, J. Zhang, Approximating a sum of random variables with a lognormal, IEEE Trans. Wirel. Commun. 6 (7) (2007) 2690–2699.

[7] W.C. Cox Jr., Simulation, Modelling, and Design of Underwater Optical Communication Systems, North Carolina State University, 2012.

[8] W. Cox, J. Muth, Simulating channel losses in an underwater optical communication system, J. Opt. Soc. Am. A 31 (5) (2014) 920–934.

[9] S.A. Thorpe, An Introduction to Ocean Turbulence, Cambridge University Press, 2007.

[10] O. Korotkova, N. Farwell, E. Shchepakina, Light scintillation in oceanic turbulence, Waves Random Complex Media 22 (2) (2012) 260–266.
[11] C. Gabriel, M.-A. Khalighi, S. Bourennane, P. Léon, V. Rigaud, Monte-Carlo-based channel characterization for underwater optical communication systems, J. Opt. Commun. Netw. 5 (1) (2013) 1–12.
[12] H. Zhang, Y. Dong, Impulse response modelling for general underwater wireless optical MIMO links, IEEE Commun. Mag. 54 (2) (2016) 56–61.
[13] H. Zhang, Y. Dong, General stochastic channel model and performance evaluation for underwater wireless optical links, IEEE Trans. Wirel. Commun. 15 (2) (2016) 1162–1173.
[14] M.V. Jamali, et al., Statistical distribution of intensity fluctuations for underwater wireless optical channels in the presence of air bubbles, in: 4th Iran Workshop on Commun. and Inf. Theory, IWCIT, IEEE, 2016, pp. 1–6.
[15] H.M. Oubei, E. Zedini, R.T. ElAfandy, A. Kammoun, M. Abdallah, T.K. Ng, M. Hamdi, M.-S. Alouini, B.S. Ooi, Simple statistical channel model for weak temperature induced turbulence in underwater wireless optical communication systems, Opt. Lett. 42 (13) (2017) 2455–2458.
[16] M.V. Jamali, A. Mirani, A. Parsay, B. Abolhassani, P. Nabavi, A. Chizari, P. Khorramshahi, S. Abdollahramezani, J.A. Salehi, Statistical studies of fading in underwater wireless optical channels in the presence of air bubble, temperature, and salinity random variations, IEEE Trans. Commun. (2018). [Online]. Available: https://ieeexplore.ieee.org/abstract/document/8370053/.
[17] M.V. Jamali, J.A. Salehi, F. Akhoundi, Performance studies of underwater wireless optical communication systems with spatial diversity: MIMO scheme, IEEE Trans. Commun. 65 (3) (2017) 1176–1192.
[18] M.V. Jamali, J.A. Salehi, On the BER of multiple-input multiple-output underwater wireless optical communication systems, in: 4th International Workshop on Optical Wireless Communications, IWOW, IEEE, 2015, pp. 26–30.
[19] Y. Dong, J. Liu, On BER performance of underwater wireless optical MISO links under weak turbulence, in: OCEANS 2016-Shanghai, IEEE, 2016, pp. 1–4.
[20] M.V. Jamali, A. Chizari, J.A. Salehi, Performance analysis of multi-hop underwater wireless optical communication systems, IEEE Photonics Technol. Lett. 29 (5) (2017) 462–465.
[21] M.V. Jamali, F. Akhoundi, J.A. Salehi, Performance characterization of relay-assisted wireless optical CDMA networks in turbulent underwater channel, IEEE Trans. Wirel. Commun. 15 (6) (2016) 4104–4116.
[22] A. Tabeshnezhad, M.A. Pourmina, Outage analysis of relay-assisted underwater wireless optical communication systems, Opt. Commun. 405 (2017) 297–305.
[23] Y. Song, W. Lu, B. Sun, Y. Hong, F. Qu, J. Han, W. Zhang, J. Xu, Experimental demonstration of MIMO-OFDM underwater wireless optical communication, Opt. Commun. 403 (2017) 205–210.
[24] Y. Chen, M. Kong, T. Ali, J. Wang, R. Sarwar, J. Han, C. Guo, B. Sun, N. Deng, J. Xu, 26 m/5.5 Gbps air-water optical wireless communication based on an OFDMmodulated 520-nm laser diode, Opt. Express 25 (13) (2017) 14760–14765.
[25] T.-C. Wu, Y.-C. Chi, H.-Y. Wang, C.-T. Tsai, G.-R. Lin, Blue laser diode enables underwater communication at 12.4 Gbps, Sci. Rep. 7 (2017) 40480.
[26] T.J. Petzold, Volume Scattering Functions for Selected OceanWaters, Tech. Rep., SIO Ref. 72–78, Scripps Institution of Oceanography Visibility Laboratory, San Diego, CA, Oct. 1972.
[27] C.D. Mobley, Light and Water: Radiative Transfer in Natural Waters, Academic press, 1994.
[28] V.V. Nikishov, V.I. Nikishov, Spectrum of turbulent fluctuations of the sea-water refraction index, Int. J. Fluid Mech. Res. 27 (1) (2000) 82–98.
[29] Y. Ata, Y. Baykal, Scintillations of optical plane and spherical waves in underwater turbulence, J. Opt. Soc. Am. A 31 (7) (2014) 1552–1556.
[30] H. Gerçekcioğlu, Bit error rate of focused Gaussian beams in weak oceanic turbulence, J. Opt. Soc. Am. A 31 (9) (2014) 1963–1968.
[31] S. Tang, X. Zhang, Y. Dong, Temporal statistics of irradiance in moving turbulent ocean, in: 2013 MTS/IEEE OCEANS-Bergen, IEEE, 2013, pp. 1–4.
[32] S.M. Navidpour, M. Uysal, M. Kavehrad, BER performance of free-space optical transmission with spatial diversity, IEEE Trans. Wirel. Commun. 6 (8) (2007) 2813–2819.
[33] L.C. Andrews, R.L. Phillips, Laser Beam Propagation Through Random Media, SPIE Press, Bellingham, WA, 2005.
[34] E.J. Lee, V.W. Chan, Part 1: Optical communication over the clear turbulent atmospheric channel using diversity, IEEE J. Sel. Areas Commun. 22 (9) (2004) 1896–1906.
[35] M. Safari, M. Uysal, Relay-assisted free-space optical communication, IEEE Trans. Wirel. Commun. 7 (12) (2008) 5441–5449.
[36] L.C. Andrews, R.L. Phillips, C.Y. Hopen, Laser Beam Scintillation with Applications, SPIE Press, 2001.
[37] M.P. Bernotas, C. Nelson, Probability density function analysis for optical turbulence with applications to underwater communications systems, in: SPIE Defense+ Security, International Society for Optics and Photonics, 2016 pp. 98270D– 98270D.
[38] R. Barrios, F. Dios, Exponentiated Weibull fading model for free-space optical links with partially coherent beams under aperture averaging, Opt. Eng. 52 (4) (2013) 046003–046003.
[39] M. Abramowitz, I.A. Stegun, Handbook of Mathematical Functions: with Formulas, Graphs, and Mathematical Tables, Courier Corporation, 1970.
[40] A.P. Prudnikov, Y.A. Brychkov, O.I. Marichev, R.H. Romer, Integrals and Series, Vol. 3: More Special Functions, Gordon and Breach Science Publishers, Amsterdam, 1986.
[41] V. Adamchik, O. Marichev, The algorithm for calculating integrals of hypergeometric type functions and its realization in REDUCE system, in: Proceedings of the international symposium on Symbolic and algebraic computation, ACM, 1990, pp. 212–224.
[42] D. Wayne, The PDF of irradiance for a free-space optical communications channel: A physics-based model (Ph.D. dissertation), School of Electrical Engineering and Computer Science, College of Engineering and Computer Science, University of Central Florida, 2010.